



Since January 2020 Elsevier has created a COVID-19 resource centre with free information in English and Mandarin on the novel coronavirus COVID-19. The COVID-19 resource centre is hosted on Elsevier Connect, the company's public news and information website.

Elsevier hereby grants permission to make all its COVID-19-related research that is available on the COVID-19 resource centre - including this research content - immediately available in PubMed Central and other publicly funded repositories, such as the WHO COVID database with rights for unrestricted research re-use and analyses in any form or by any means with acknowledgement of the original source. These permissions are granted for free by Elsevier for as long as the COVID-19 resource centre remains active.



Identifying potential human and medicinal plant microRNAs against SARS-CoV-2 3'UTR region: A computational genomics assessment

Naman Mangukia^{a,c}, Priyashi Rao^b, Kamlesh Patel^d, Himanshu Pandya^a, Rakesh M. Rawal^{b,*}

^a Department of Botany, Bioinformatics and Climate Change Impacts Management, School of Sciences, Gujarat University, Ahmedabad, 380009, Gujarat, India

^b Department of Biochemistry and Forensic Science, University School of Sciences, Gujarat University, Ahmedabad, 380009, Gujarat, India

^c BioInnovations, Bhayander (West), Mumbai, 401101, Maharashtra, India

^d Advait Theragnostics, GUSEC, Gujarat University, Ahmedabad, 380009, Gujarat, India

ARTICLE INFO

Keywords:

Computational genomics

miRNA

SARS-CoV-2

Conserved 3'UTR

Antiviral defense

Medicinal plants

ABSTRACT

The coronavirus disease of 2019 (COVID-19) began as an outbreak and has taken a toll on human lives. The current pandemic requires scientific attention; hence we designed a systematic computational workflow to identify the cellular microRNAs (miRNAs) from human host possessing the capability to target and silence 3'UTR of SARS-CoV-2 genome. Based on this viewpoint, we extended our miRNA search to medicinal plants like *Ocimum tenuiflorum*, *Zingiber officinale* and *Piper nigrum*, which are well-known to possess antiviral properties, and are often consumed raw or as herbal decoctions. Such an approach, that makes use of miRNA of one species to interact and silence genes of another species including viruses is broadly categorized as cross-kingdom interactions. As a part of our genomics study on host-virus-plant interaction, we identified one unique 3'UTR conserved site 'GGAAGAG' amongst 5024 globally submitted SARS-CoV-2 complete genomes, which can be targeted by the human miRNA 'hsa-miR-1236-3p' and by *Z. officinale* miRNA 'zof-miR2673b'. Additionally, we also predicted that the members of miR477 family commonly found in these three plant genomes possess an inherent potential to silence viral genome RNA and facilitate antiviral defense against SARS-CoV-2 infection. In conclusion, this study reveals a universal site in the SARS-CoV-2 genome that may be crucial for targeted therapeutics to cure COVID-19.

1. Introduction

The coronavirus disease of 2019 (COVID-2019) began as an outbreak in Wuhan, China in late 2019 and shook the world which led the World Health Organization (WHO) to declare it as a global pandemic in March 2020 [1,2]. The WHO statistics indicate that people affected by COVID-19 has surpassed 187 million among which worldwide mortality of 4.04 million recorded around July 14, 2021. If recent events are any indicators of the epidemics of the past, the rapid spread of this viral disease reflects that the antidote to this pandemic is not by self-isolation but by envisaging strategies to overcome and minimize the critical situation. The need of the time during this pandemic is to develop strategies to curb SARS-CoV2 using a scientific approach. The obvious choice is the use of vaccines however, the vaccine deployment process has its limitations, which is further hindered by civilians refraining to get vaccinated. Vaccines, in fact, do not minimize or eradicate the virus but

helps boost the immune response against a specific viral serotype which may be ineffective against another serotype [3]. Therefore, global scientists are challenged to find an alternative strategy that directly targets the functioning of the viral particle. For such an approach, either inhibitors of SARS-CoV-2 structural proteins and enzymes are to be developed [4–6], or the viral genome functional integrity to be targeted making use of microRNAs (miRNAs).

SARS-CoV-2 as named by the International Committee on Taxonomy of Viruses (ICTV), is a single-stranded positive-sense RNA virus of the Coronaviridae family with a genome size of 26–32 kb [7] and comprises 14 open reading frames (ORFs) encoding 27 polyproteins. The first ORF comprises approximately 67% of the genome that encodes 16 non-structural proteins (nsps), whereas the remaining ORFs encode for accessory and structural proteins called the spike (S) glycoprotein, envelope (E), membrane (M) and nucleocapsid (N) proteins which are the focal target proteins for drug repurposing and therapeutics studies. The

* Corresponding author.

E-mail addresses: namanmangukia@gujaratuniversity.ac.in (N. Mangukia), priyashi.rao@gujaratuniversity.ac.in (P. Rao), kamlesh.patel@advaitdx.com (K. Patel), hapandya@gujaratuniversity.ac.in (H. Pandya), rakeshrawal@gujaratuniversity.ac.in (R.M. Rawal).

<https://doi.org/10.1016/j.complbiomed.2021.104662>

Received 16 May 2021; Received in revised form 15 July 2021; Accepted 15 July 2021

Available online 19 July 2021

0010-4825/© 2021 Elsevier Ltd. All rights reserved.

SARS-CoV-2 genome also has two flanking untranslated regions (UTRs) at 5' end of 265 nucleotides and 3' end of 358 nucleotides [8,9]. All kinds of viruses including the SARS-CoV-2, multiply within the host cell by hijacking the nucleic acid synthesis machinery as well as the protein translation system because information travels from the genome to ultimately encode a functional protein in the molecular interplay of the central dogma. If this functionality of the virus is silenced then their proteins would not be formed and the viral life will not be able to thrive inside the human host which ultimately leads to apoptosis of the infected cell [10]. For consolidating the rationale of current research, there exist substantial evidence revealing that miRNA whether present endogenously inside the host or acquired exogenously through diet, possess the ability to interact with the 3'UTR flanking region based on complementarity to the target mRNA [11–13] and mediate translational repression or mRNA degradation thereby shutting off the viral system [14].

miRNA forms a class of non-immunogenic, single-stranded non-coding RNAs of approximately 22 nucleotides, that play a significant role in regulating the gene expression at the post-transcriptional level and is an integral part of a eukaryotic cell. miRNAs that are endogenously found in human cells are called 'cellular miRNAs' while those acquired by consuming vegetable-based plant food are simply addressed as 'plant miRNAs'. The majority of miRNAs are transcribed from DNA sequences into primary miRNAs and form precursor miRNAs and finally transform into mature miRNAs. In most cases, miRNAs interact with the 3' UTR of the target mRNAs causing translational repression or mRNA degradation to block the mechanism of protein translation [10,14]. The first miRNA 'lin-4' was identified from *Caenorhabditis elegans* [15] and subsequently, miRNAs in the range of organisms from plants to humans have been identified. Currently, according to the miRBase database [16, 17], there are in total 48,885 mature miRNAs present of which 437, 469, 2656 and 10,414 mature miRNA entries belong to organisms *C. elegans*, *Drosophila melanogaster*, *Homo sapiens* and plants respectively, with each of these miRNAs having a potential to regulate different target genes of the viral transcripts [10].

When we consume plants, along with them we also consume their genetic material and nucleic acids, of which miRNAs are also a part. As mentioned earlier, plant miRNAs interact with nucleic acids (like mRNA) present in human cells which form the fundamental grounds of cross-species interaction. As more exogenous miRNAs of plants were experimentally observed in humans, the modulation of any human gene by miRNAs of plants was unknown until Zhang and colleagues in 2012 discovered the role of plant miRNA as universal modulators of human genes and helped understand their role in plant-human crosstalk at a molecular level. Further, these miRNAs can also modulate viral gene expression residing in infected host cells [13,18]. For instance, a plant-derived miRNA designated as 'miRNA2911' suppressed the expression of Influenza A virus in mice. This finding was the first of its kind suggesting that plant-derived miRNA can impart implications to the animal infected with the virus. It is also observed that regular oral administration of honeysuckle decoction can suppress the pathogenicity of the Influenza A viral infection [19]. Subsequent studies revealed that plant miRNAs bearing 2'-O-methylated 3' ends could stably exist in the sera as well as tissue of humans and herbivorous animals. They are stable and resistant to enzymatic digestion in the highly acidic environment of gastrointestinal tract and could selectively be packaged into microvesicles (MVs) and specifically delivered to the recipient cells, where based on the complementarity between the miRNA and its 3' UTR site it can block protein translation or carry out degradation of the mRNAs on the target genes [13,20,21]. The research group that worked on the oral administration of Honeysuckle decoction extended its application to a clinical study with COVID-19 patients to study the decoction efficacy in mitigating the conditions of COVID-19. They found that plant miRNA2911 was sufficiently absorbed and possesses inhibitory activity against SARS-CoV-2 viral replication [22]. Globally, many research groups are making progressive efforts to establish the

significant contribution of natural products from spices and herbs as a means of prevention and control from SARS-CoV-2 infection. Recently, a randomized placebo-controlled pilot preclinical trial showed rapid improvement in clinical symptoms with no adverse secondary infection upon periodic consumption of *Z. officinale* tablets by patients infected with SARS-CoV-2 [23]. Another report suggested the use of bioactive compounds like curcumin, allicin and gingerol as an effective treatment regime to cure viral infection [24]. Concluding literature, it can be fairly stated that endogenous cellular miRNAs and acquired exogenous plant miRNAs from a plant-based diet, can bind to the 3'UTR flanking region based on complementarity to the target mRNA and significantly suppress the viral pathogenicity. These findings thereby provide many opportunities and strategies to explore the cross-kingdom network of virus-host-plant by identifying probable miRNA candidates to target the SARS-CoV-2 virome. The identified antiviral miRNA could potentially act as a therapeutic agent to treat the viral SARS-CoV-2 infection and may help in managing comorbidities. In this study, we designed a systematic computational workflow as explained in Fig. 1, to explore the human host miRNA-virus interaction and identified probable cellular miRNA candidates which might be involved in mediating viral mRNA silencing and thus, may play a pivotal role in providing antiviral defense against SARS-CoV-2 infection. This study also investigates the cross-species interaction of medicinal plant miRNAs with the SARS-CoV-2 virus, we selected those medicinal plants that are often associated with immune-boosting properties and are either consumed raw or in form of decoction.

This study aims to identify the probable miRNA candidates from three medicinal plants namely, *O. tenuiflorum*, *Z. officinale* and *P. nigrum* that are associated to possess antiviral properties.

2. Material and methods

2.1. Sequence retrieval and filtration of SARS-CoV-2 genomes

SARS-CoV-2 genome sequence was retrieved from NCBI (National Centre for Biotechnology Information) (GenBank accession: NC_045512.2) [1] and was used as a reference genome of SARS-CoV-2 throughout the study. The reference genome sequence is marked by three features, namely: 5'UTR (1–265), CDS (266–29674) and 3'UTR (29,675–29903), depicted in Fig. 2A.

The 3'UTR region of SARS-CoV-2 genome is the focus of this study; therefore, it was mandatory to identify variations in the 3' UTR region of SARS-CoV-2. All the sequences were retrieved in fasta format from NCBI and GISAID (Global Initiative on Sharing All Influenza Data) [25] repositories as of 4th October 2020. To obtain the complete genome sequence, length (>29,900) and filtering criteria (No n/N and hyphen in the sequence) were applied and an in-house Perl script was used to fetch 3'UTR regions as described in Fig. 2B. Detailed information regarding the complete collection of retrieved SARS-CoV-2 genome sequences and fetched 3'UTR regions are provided in the supplementary material and its country-wise distribution in Supplementary-Table 1.

2.2. Determining conserveness of 3'UTR sequence

To explore the global variation amongst all the fetched 3'UTR sequences deposited in the NCBI and GISAID databases, Multiple Sequence Alignment (MSA) was performed using Clustal Omega (standalone version:1.2.4) [26] with default parameters on 3'UTR stretches of SARS-CoV-2 genome. Before performing the MSA, a 3'UTR region of the SARS-CoV-2 reference genome (NC_045512.2:29,675–29870) was added to GISAID dataset for the purpose of comparative analysis of MSA result with NCBI dataset as shown in Fig. 2C.

2.3. Targeting human mature miRNA sequences on 3'UTR

To investigate the cross-species interaction involving human miRNA-

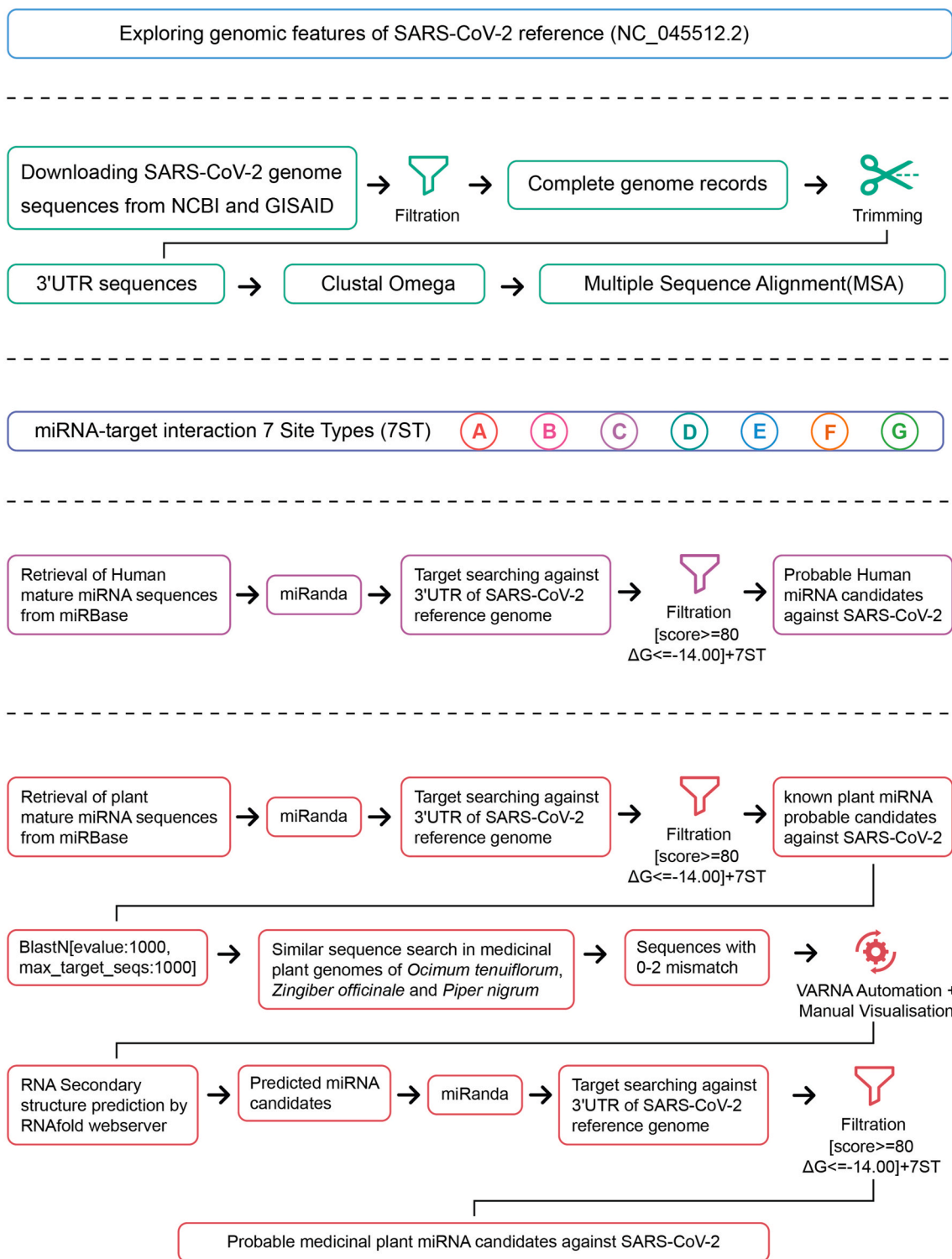


Fig. 1. A systematic workflow of the study.

virus 3'UTR, all mature human miRNA sequence entries were retrieved from the miRBase repository (release 22.1: October 2018) [17,27] in fasta format and were screened against SARS-CoV-2 3'UTR region using miRanda algorithm (standalone version:3.3a) and the obtained hits were filtered on the basis of hybridization alignment score ≥ 80 and minimum energy of $\Delta G \leq -14$ kcal/mol for the miRNA: 3'UTR duplex structure [28]. The obtained hits were further filtered according to the seven types of sites proposed by Bartel (2009) graphically illustrated in Fig. 3 [12].

2.4. Prediction of medicinal plant miRNAs and targeting them to 3'UTR

Based on the availability of the draft genomes, this study is focused on three medicinal plants namely, *O. tenuiflorum*, *Z. officinale* and *P. nigrum*. However, due to the unavailability of the miRNA sequences of these three medicinal plants in the miRBase repository; it was first necessary to predict the 3'UTR targets of known mature plant miRNA entries available in miRBase. Similar to above steps used to screen human miRNAs using miRanda algorithm, the 3'UTR region of SARS-

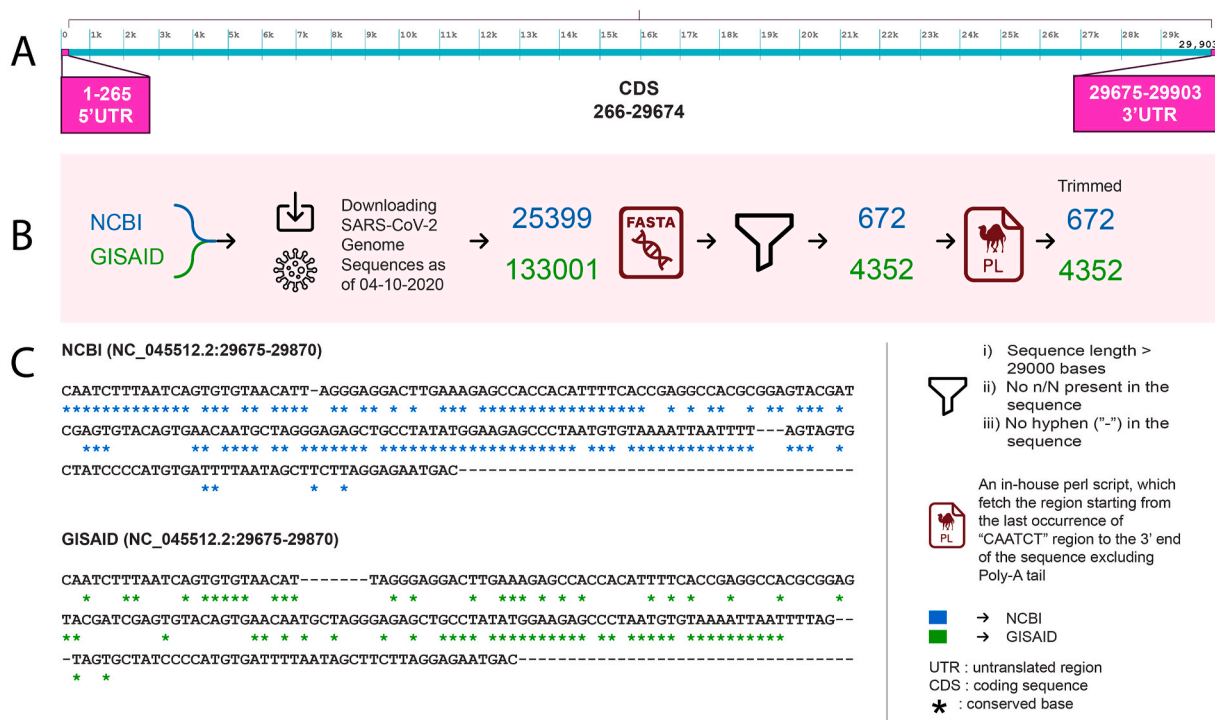


Fig. 2. (A) Genomic features of SARS-CoV-2 reference genome (NC_045512.2): UTR (Untranslated region) and CDS (Coding sequence). Each feature has been shown with its spanning region length. The scale representing the genome is having the unit of 1k (1000) bases. (B) SARS-CoV-2 Genome sequences (as of 4th-Oct-2020) retrieval procedure: This section represents download, filtration and trimming steps to capture 3'UTR sequences from the downloaded sequence records, excluding Poly-A tail. In procedure-flow, the blue and green colour represents the figure and facts regarding NCBI and GISAID repositories respectively. 'Filtration' and 'In-house Perl script' icons are explained stepwise in the right-side panel. (C) MSA (Multiple Sequence Alignment): This section shows MSA results, performed on 3'UTR of SARS-CoV-2 genomes for NCBI and GISAID datasets individually. Both NCBI and GISAID MSA results are represented by the SARS-CoV-2 reference genome (NC_045512.2) 3'UTR (length:196 bases) region. "*" denotes conservensness of the respective base. "-" represent gap in the alignment. The combined NCBI and GISAID MSA result (without gaps) along with their conservensness denotation (*) will be used throughout this study.

Table 1
MFEI values of predicted miRNA precursors.

Predicted miRNAs	MFE	MFEI
pni-miR477d-5p	-47.23	-1.21
zof-miR477e	-60.06	-0.94
ote-miR477h	-65.00	-1.14
ote-miR169e-3p	-96.20	-1.15
zof-miR2673b	-116.13	-0.87

CoV-2 reference genome was targeted by the plant miRNAs. The obtained plant miRNA sequences having 3'UTR complementarity were screened through the whole genomes of the three medicinal plants using Blastn (standalone Blast-version 2.10.0+) program [29,30] with an e-value of 1000 and maximum target sequence set to 1000 parameters. The genome sequences of *O. tenuiflorum* (INSDC ID: AYJT00000000.1) and *Z. officinale* (INSDC ID: WXZB00000000.1) were retrieved from NCBI while the *P. nigrum* genome sequence was obtained from the database of The Group of Cotton Genetic Improvement (GCGI) (<http://cotton.hzau.edu.cn/EN/download.php>).

The resulted hits with a minimum of two substitutions (including gap and mismatches) on the genomic region were fetched together with their flanking region up to 350 bases. An in-house Perl script automation utilizing mfold (standalone version 3.6) [31] and VARNA [32] was applied on these captured regions, which retrieved the predicted RNA secondary structures that fulfilled the following criteria [33–37] including i. The miRNA sequences with breaks or loops were circumvented, ii. the minimum length of predicted mature miRNA was 18 nucleotides, ii. Only 0–2 mismatches were allowed between predicted and known homologue mature miRNA sequence alignment portion, iv.

The predicted precursor miRNA structure must be folded into a near-perfect or perfect stem-loop hairpin secondary structure, v. No more than 6 nucleotide mismatches in miRNA/miRNA* duplex were permitted, vi. Predicted mature miRNA sequence located in any one arm of the hairpin structure, vii. Predicted mature miRNA sequence must be in the same arm as its plant homologue, vii. Predicted precursor miRNA sequence having a length of minimum 60 nucleotides, ix. Predicted precursor miRNAs must have a higher negative MFEI (Minimum Folding free Energy Index) value. The calculation of MFEI values was performed using the following formula [38]:

$$MFEI = ((MFE \div \text{length of RNA sequence}) * 100) / (G + C) \%$$

Where MFE is a Minimum Free Energy (ΔG in kcal/mol) calculated by RNAfold webserver [39].

The final predicted structure was cross validated using online mfold webserver [31] and pre-miRNA secondary structures were drawn using RNAfold webserver [39]. In addition, the mature plant miRNA sequences corresponding to these structures were identified and screened against 3'UTR region of SARS-CoV-2 reference genome.

3. Results

3.1. Conservational analysis of SARS-CoV-2 3'UTR sequence

A total of 25,399 and 1,33,001 SARS-CoV-2 genome sequence records were retrieved from NCBI and GISAID, respectively. As depicted in Fig. 2B, these sequences were trimmed and refined to obtain 3'UTR region. A total of 5024 sequences 3'UTR region were used in this study of which 672 sequences belongs to NCBI and 4352 sequences to GISAID.

To explore the global variation amongst all the 3'UTR sequences

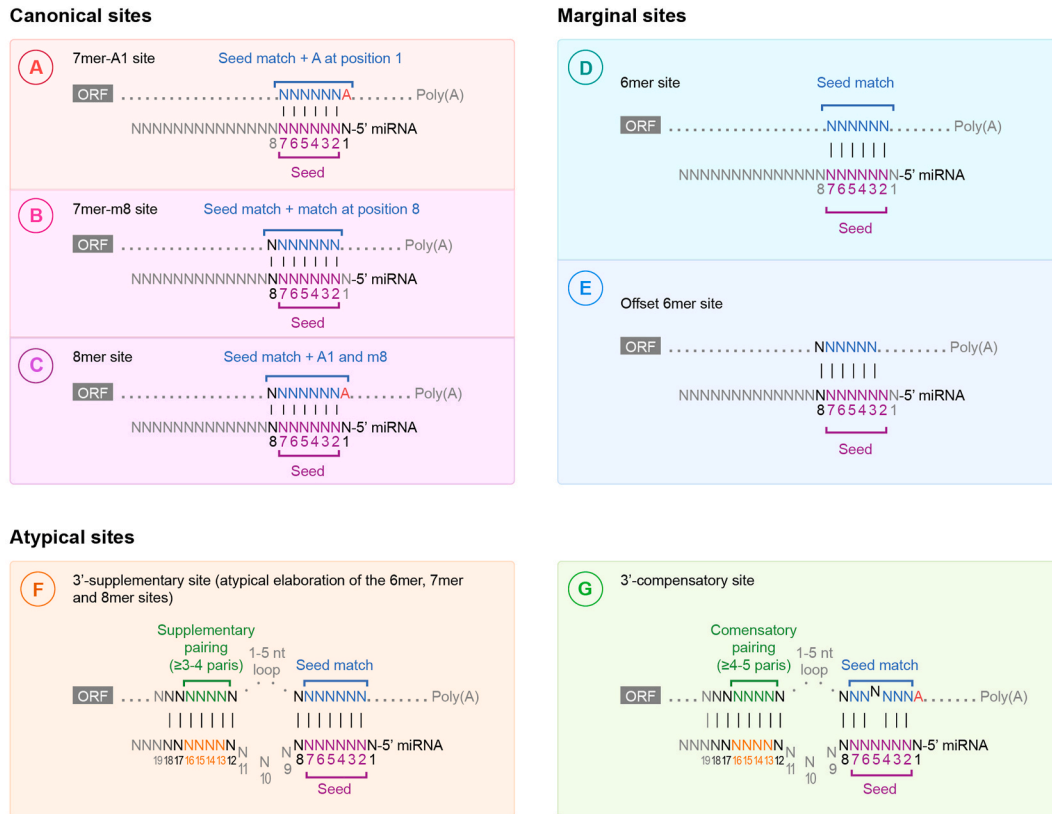


Fig. 3. Site-types of miRNA-Target interactions: A total of 7 site types were depicted in this section, adapted from Bartel (2009) [12].

deposited in the NCBI and GISAID databases, we performed MSA using Clustal Omega with default parameters on the 3'UTR stretches of SARS-CoV-2 genome. MSA was performed individually for NCBI and GISAID dataset. The 196 bases long 3'UTR region of SARS-CoV-2 reference genome was set as the reference for MSA and the subsequent alignments were fetched out from the entire MSA result for NCBI and GISAID as depicted in Fig. 2C. The "*" indicates the conserveness of the base just above its denotation. In other words, the bases with "*" denotation are conserved or 100% stable amongst the datasets. The representative initial 13 bases "CAATCTTTAATCA" are denoted by "*" in NCBI alignment (Fig. 2C) suggesting that they are conserved throughout the 672 NCBI sequences. Likewise, considering these initial 13 bases in GISAID alignment, only the 2nd, 7th, 8th and 13th bases are conserved amongst all 4352 sequences.

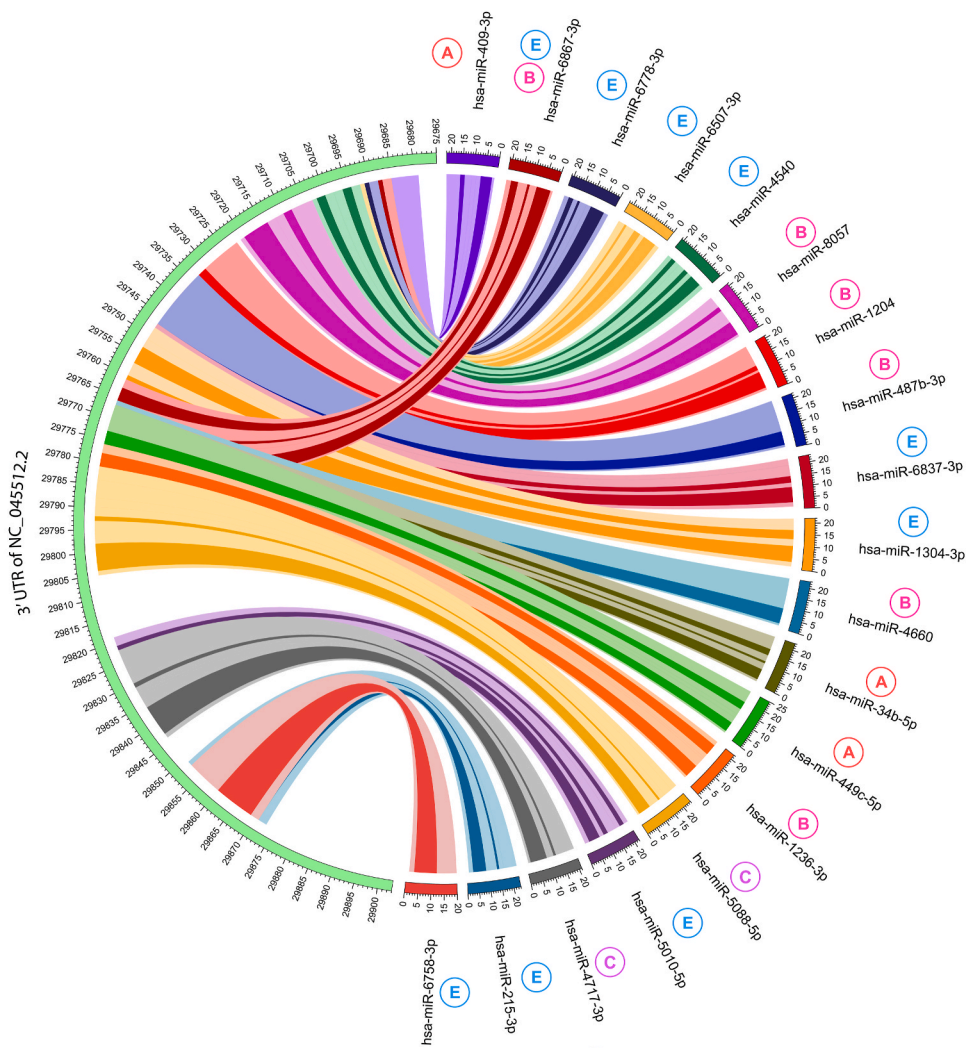
A total of 9 conserved nucleotide stretches were observed from both NCBI and GISAID MSA analysis. Out of which five conserved nucleotide stretches belong to NCBI retrieved sequences (i:29,675–29687, ii:29,716–29732, iii:29,779–29784, iv:29,786–29805 and v:29,811–29826). Likewise, four conserved nucleotide stretches (i:29,689–29693, ii:29,791–29800, iii:29,805–29809 and iv:29,811–29820) were found in GISAID representative alignment. Conserved nucleotide stretches include a minimum of 5 continuous conserved nucleotides which are the probable miRNA binding sites. Minimum five bases "complementarity" match was also required in site-types [12] as mentioned in Fig. 3. Amongst these 9 conserved regions of NCBI and GISAID, 2 common nucleotide stretches were observed: region-i:29,791–29800 (conserved nucleotide stretch-iv from NCBI and ii from GISAID) and region-ii:29,811–29820 (conserved nucleotide stretch-v from NCBI and iv from GISAID). These two nucleotide stretches are conserved across all the 5024 3'UTR of SARS-CoV-2 sequences, which are potential targets for miRNA. Individually, 123 (62.75%) bases are conserved in NCBI, and 84 (42.85%) bases are conserved in GISAID alignments. A total of 67 common conserved bases were found from both NCBI and GISAID

alignments. The percentage (%) base-stability was calculated for all 196 bases of 3'UTR of SARS-CoV-2 reference genome, provided in Supplementary Table- 2 for NCBI and GISAID alignments separately. Here, the "base-stability" refers to the frequency of any representative base for its respective position in MSA. All conserved bases are having 100% base-stability. In the non-conserved region, the base "C" at position 29, 870 was found with minimum base-stability (93.1%) and the base "G" at position 29,688 was found with maximum base-stability (99.8%) for NCBI alignment, while for GISAID alignment, the base "G" at position 29,868 was found with minimum base-stability (95.7%) and there were 67 bases were found with maximum base-stability (99.9%). The overall base-stability rate for the 3'UTR region of all the sequences is 99.76% and 99.79% for NCBI and GISAID respectively. These 9 nucleotide stretches were observed to be conserved amongst all the repositd sequences of SARS-CoV-2 from both the databases allowing us to predict that these stretches can act as stipulated sites and can potentially be targeted to regulate the post-transcriptional events of the SARS-CoV-2 lifecycle.

3.2. Identification of potential human miRNA candidates

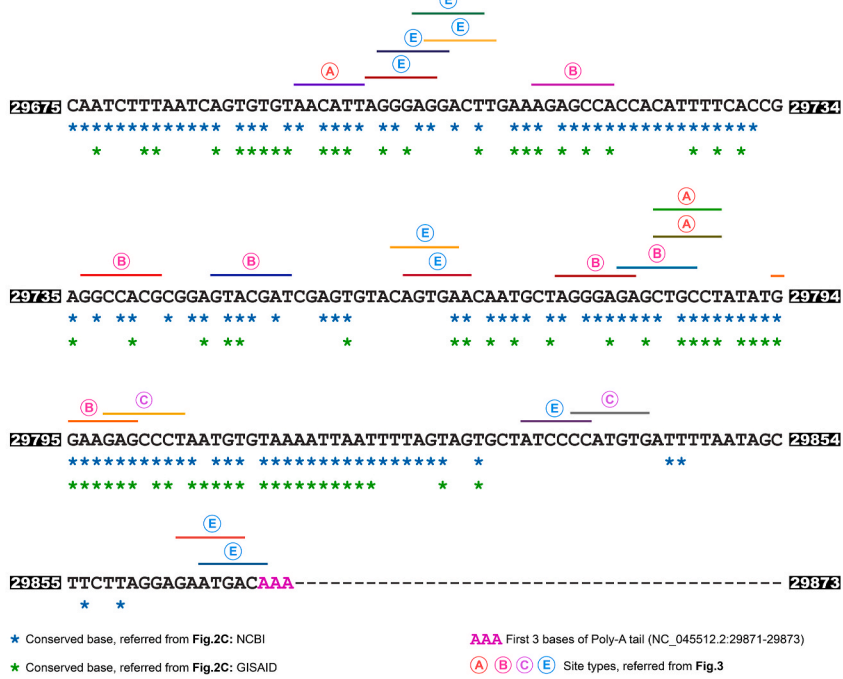
A complementary search of 2656 known human mature miRNA sequences against SARS-CoV-2 reference genome 3'UTR was performed using miRanda algorithm. Taking into account the filtration and site-types [12] criteria, predominantly 20 hits by 19 miRNA candidates namely: hsa-miR-409-3p, hsa-miR-6867-3p, hsa-miR-6778-3p, hsa-miR-6507-3p, hsa-miR-4540, hsa-miR-8057, hsa-miR-1204, hsa-miR-487b-3p, hsa-miR-1304-3p, hsa-miR-6867-3p, hsa-miR-4660, hsa-miR-34b-5p, hsa-miR-449c-5p, hsa-miR-1236-3p, hsa-miR-5088-5p, hsa-miR-5010-5p, hsa-miR-4717-3p, hsa-miR-215-3p and hsa-miR-6758-3p were observed. The human miRNAs and their respective aligned region of 3'UTR are depicted in Fig. 4A using Circos [40] representation and MSA in Fig. 4B. The free energy (ΔG) ranges

A



B

- 1 hsa-miR-409-3p
● cloned, array-cloned
 - 2 hsa-miR-6867-3p
● meta-analysis
 - 3 hsa-miR-6778-3p
● meta-analysis
 - 4 hsa-miR-6507-3p
● illumina
 - 5 hsa-miR-4540
● illumina
 - 6 hsa-miR-8057
● illumina
 - 7 hsa-miR-1204
● Northern
 - 8 hsa-miR-487b-3p
● cloned, illumina
 - 9 hsa-miR-6837-3p
● meta-analysis
 - 10 hsa-miR-1304-3p
● illumina
 - 11 hsa-miR-4660
● illumina
 - 12 hsa-miR-34b-5p
● M0000404
 - 13 hsa-miR-449c-5p
● RAKE, 454
 - 14 hsa-miR-1236-3p
● cloned
 - 15 hsa-miR-5098-5p
● illumina, qPCR, meta-analysis
 - 16 hsa-miR-5010-5p
● illumina
 - 17 hsa-miR-4717-3p
● illumina
 - 18 hsa-miR-215-3p
● cloned, illumina
 - 19 hsa-miR-6758-3p
● meta-analysis
- Evidence by miRBase
● Experimental ● By similarity



(caption on next page)

Fig. 4. (A) Circos representation: 19 human miRNA and their respective 20 targets on 3'UTR of SARS-CoV-2 reference genome (NC_045512.2) depicted using ribbon connection by Circos diagram. The single outer layer of Circos diagram was divided into 2 main sections: 1) Human miRNAs and 2) 3'UTR of SARS-CoV-2 reference genome. The circular layer is having a scale bar that represents the length of the respective entity (miRNA/3'UTR). Each human miRNA is tagged by the respective site type (as mentioned in Fig. 3). Each alignment between human miRNA and SARS-CoV-2 3'UTR region is represented by coloured-ribbon, where the specific colour is assigned according to the human miRNA series mentioned in bottom-left section B. The dark colour stroke in each ribbon shows the complementary match between the respective human miRNA and SARS-CoV-2 3'UTR bases. (B) Alignment with the global MSA result perspective: In this section, the combined MSA result of 3'UTR belonging to NCBI and GISAID datasets using the respective conserveness (Blue *: NCBI; Green *: GISAID) denotation is shown. The horizontal lines above the SARS-CoV-2 3'UTR bases (29,675–29873 including initial 3 poly-A tail residues) represent its complementary matching region with the respective human miRNA along with the site type. As mentioned, each human miRNA is assigned with a specific colour denoted in series number at the bottom-left panel, the respective horizontal colour line placed on the MSA result can be identified using it. Each human miRNA is provided with evidence from the miRBase repository.

from -26.31 to -14.01 and match score range is from 140 to 155 of the 20 resulted human miRNA-viral 3'UTR alignments. The detailed information is provided in [Supplementary Fig. 1](#).

Further, hsa-mir-6867-3p is having 2 seed match regions targeting 3'UTR of SARS-CoV-2 and these are (i) Target site-1: AGGGAG (29,700–29705) and (ii) Target site-2: AGGGAGA (29,776–29781). Given that complementarity amongst the human miRNA and 3'UTR is the key factor in determining the cross-species interaction, it becomes crucial to identify a common nucleotide stretch that is conserved amongst the 3'UTR region of all 5024 SARS-CoV-2 sequences. One such nucleotide stretch was identified having the sequence "GGAAGAG" (29,794–29800) and this sequence was observed to be targeted by only one miRNA known as hsa-miR-1236-3p. Hence, out of 2565 known human miRNA hsa-miR-1236-3p was identified as the most effectively interacting with the 3'UTR region of SARS-CoV-2.

3.3. Identification of potential plant miRNAs from three medicinal plants

Predicting all miRNAs from three selected plant genomes and then finding their targets on 3'UTR is a laborious process generating thousands of similar hits altering the entire process and therefore to overcome this, the entire 10,414 known plant miRNA sequences from miRBase were searched against 3'UTR of SARS-CoV-2 reference genome using miRanda software.

The screening resulted in 69 non-redundant (nr) hits. The 69 plant miRNAs were screened through entire draft genomes of *O. tenuiflorum*, *Z. officinale* and *P. nigrum*. A total of five potential miRNA candidates were predicted from the three medicinal plants: two miRNAs from *O. tenuiflorum* (ote-miR477h and ote-miR169e-3p), two miRNAs from *Z. officinale* (zof-miR477e and zof-miR2673b) and pni-miR477d-5p from *P. nigrum*. The precursor structures of predicted plant miRNA are depicted in [Fig. 5A](#). The minimum free energy (ΔG) value of these miRNA precursor structures lies in the range of -116.23 kcal/mol to -47.23 kcal/mol and the MFEI values lie in the range of -1.21 to -0.87 . The MFE and MFEI values of all 5 miRNA precursor structures are given in [Table 1](#). The general features of predicted miRNAs are described in [Fig. 5B](#).

These five predicted mature sequences were then screened against 3'UTR of SARS-CoV-2 reference genome and resulted in five hits. The free energy (ΔG) and match score were calculated using miRanda program for plant miRNA-viral 3'UTR alignments. The ΔG of these alignments range from -26.68 kcal/mol to -17.45 kcal/mol and match score range is from 140 to 152. The detailed information is provided in [Supplementary Fig. 2](#).

The miRNA, pni-miR477d-5p, ote-miR477h and zof-miR477e are observed to share the same binding site region "GGGAGA" (29,777–29782) where the binding site for pni-miR477d-5p and zof-miR477e is "AGGGAGA" (29,776–29782) while binding site "GGGAG" (29,777–29783) corresponds to that of ote-miR477h. While the miRNA, zof-miR2673b targeting the binding site "GGAAGAG" (29,794–29800) is found to be conserved amongst all the 5024 3'UTR region of SARS-CoV-2 sequences belonging to NCBI and GISAID databases. Sequence alignments amongst five plant miRNAs and 3'UTR of SARS-CoV-2 reference genome are provided in [Supplementary Fig. 2](#).

Binding of *Z. officinale* miRNA: zof-miR2673b at a conserved site on

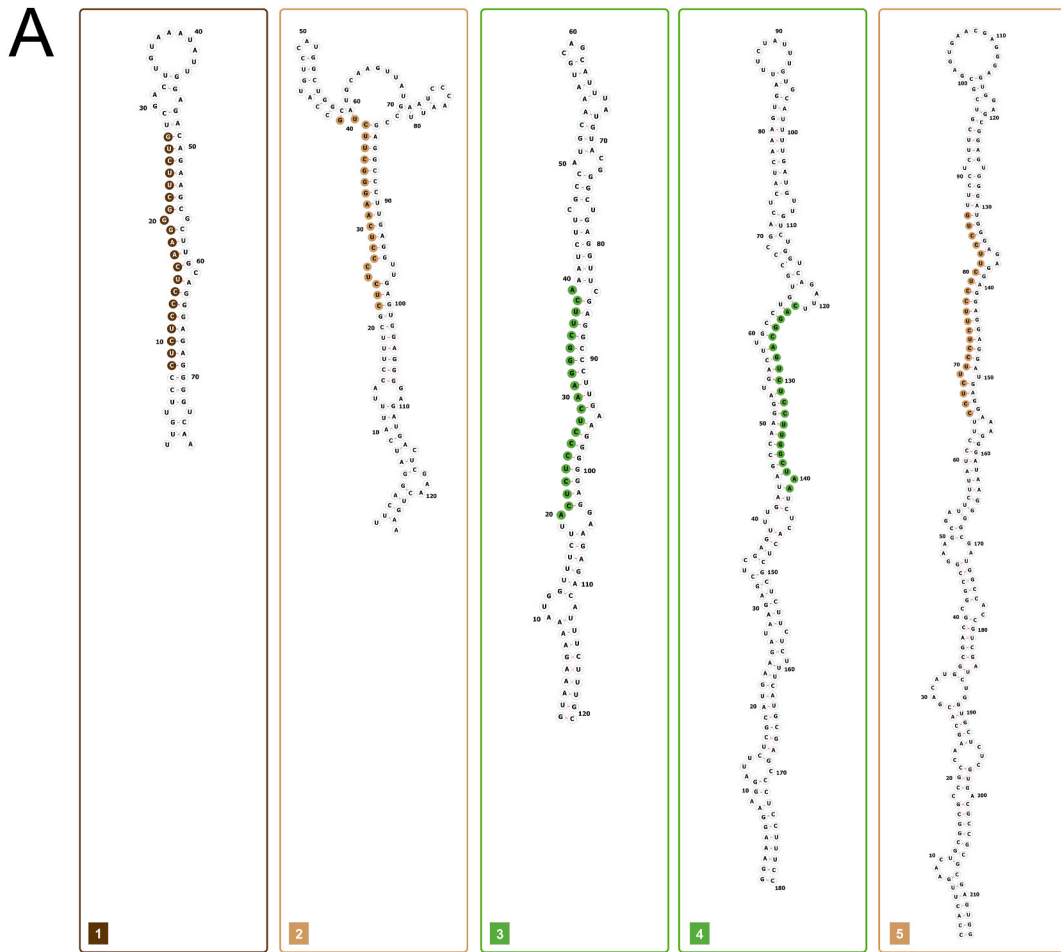
the 3'UTR suggests the possibility that *Z. officinale* produces a notable zof-miR2673b belonging to the family of miR2673 which can potentially bind and modulate the repression or degradation of viral elements. Moreover, the five predicted miRNAs belong to the family of miR477, miR 169 and miR2673. One of the noteworthy findings was that the miR477 family was found to be common amongst these predicted plant miRNAs becoming a miRNA candidate of prominence. However, further research to gain a better perspective on the role of these miRNAs is required.

4. Discussion

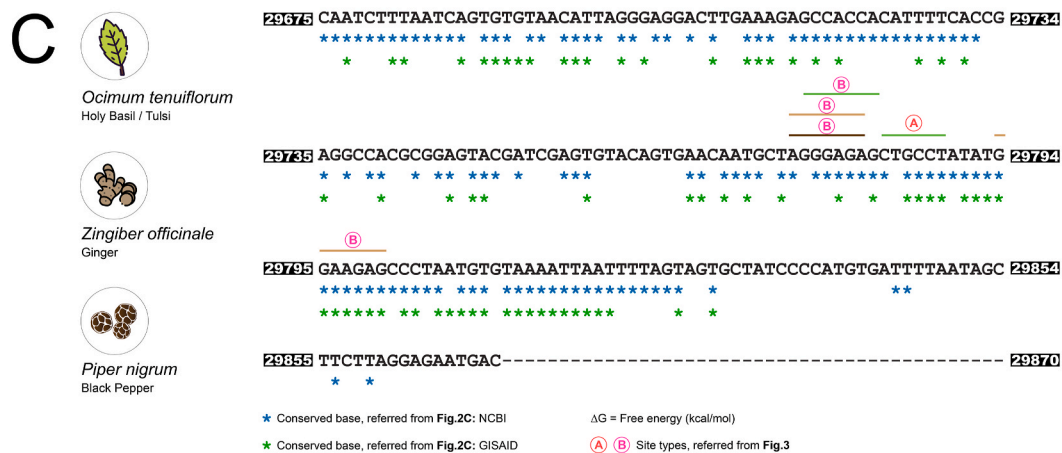
There are numerous studies in which miRNAs are known to modulate a virus-human-plant cross kingdom interplay. Firstly, taking into consideration the cross-species interplay of virus and human host, two miRNAs namely, miR-221 and miR-222 are observed to regulate CD4 surface protein in case of acquired immunodeficiency syndrome (AIDS) caused by Human Immunodeficiency Virus (HIV) [41]. Similarly, miR-34, miR-15, and miR-517 families of miRNA are known to generate an antiviral response in multiple diseases caused by flavivirus infection [42]. While let-7, miR-25 and miR-130 families are known to repress essential Hepatitis C Virus (HCV) proteins at various stages of the viral lifecycle thus restricting viral infection [43]. This has provided a new outlook on the diagnosis and treatment of viral diseases. The second crucial factor of miRNA-mediated cross-species interaction is the virus-plant interplay wherein plant miRNA displays an antiviral response [44,45]. Plant miRNAs like pre-miR 159 were studied first in *Arabidopsis thaliana* against Turnip yellow mosaic virus (TYMV) [46], Turnip mosaic virus (TuMV) [47] and CMV [48]. Besides, numerous reports suggest the role of heightened antiviral defense against rice stripe virus (RSV) through suppression of miR 528 miRNA found in *Oryza sativa* [49].

Another cross-species network interaction involves the role of plant miRNAs in human diseases. The first breakthrough of studying the cross-species interaction of plant miRNAs and human genes made by Zhang and his group had promoted the strategy to examine the feasibility of plant miRNAs to target human genes through the consumption of plants as diet [13,18]. For example, miRNA2911 from *Lonicera japonica* decoction on select subtypes of Influenza A virus-infected mice and also on SARS-CoV-2 viral infection [19,22]. Similarly, oral administration of *Adhatoda Vasica* extract (AV), an ayurvedic medicine was experimentally proven to have anti-hypoxic and anti-inflammatory properties with the ability to reduce severe airway inflammation in COVID-19 affected patients [50].

The medicinal plants we explored in this study, *Z. officinale* and *P. nigrum*, are known to possess anti-cancer activity [51], anti-inflammatory and anti-tuberculosis activities [52]. Promising antiviral efficacy of *Ocimum sanctum* leaf extracts against Avian influenza H9N2 infection was revealed in the embryonated egg model [53]. Similarly, the antiviral efficacy of *Z. officinale* extract against the Chikungunya virus [54] and human respiratory syncytial virus (HRSV) were studied which suggested that fresh ginger in high concentration could stimulate IFN- β production from mucosal cells to vesical suppress HRSV infection [55]. Various experimental evidence documented the potential of antioxidant, anti-mutagenic, anti-bacterial, anti-tumor,



Sr. No.	miRNA	Homologous miRNA	Source					Precursor ΔG (kcal/mol)
			Organism	Scaffold/Chromosome	Strand	Mature Position	Precursor Position	
1	pni-miR477d-5p	csi-miR477d-5p	Piper nigrum	Pn5	+	8233363-8233382	8233356-8233431	-47.23
2	zof-miR477e	mes-miR477e	Zingiber officinale	WXZB01734495.1	+	43-62	22-146	-60.06
3	ote-miR477h	mes-miR477h	Ocimum tenuiflorum	AYJT01101310.1	+	8774-8793	8755-8875	-65.00
4	ote-miR169e-3p	csi-miR169e-3p	Ocimum tenuiflorum	AYJT01073879.1	+	6004-6023	5883-6062	-96.20
5	zof-miR2673b	mtr-miR2673b	Zingiber officinale	WXZB01002640.1	-	7336-7317	7400-7187	-116.13



(caption on next page)

Fig. 5. (A) Secondary structure prediction: This section depicts RNAfold predicted 5 miRNA precursor secondary structures from 3 medicinal plants - *Ocimum tenuiflorum*, *Zingiber officinale* and *Piper nigrum*. Each precursor structure is provided with a serial number at the bottom, as defined in section B. (B) This tabular-view section represents the information regarding the newly predicted 5 miRNAs. Column-1 is a serial number, and each serial number is having an organism-specific colour, which is used to pinpoint the respective information: i) Mature miRNA sequence region is highlighted with the respective colour inside each precursor structure given in section-A. ii) Horizontal lines with the respective organism colour given in section C. Column-2 represents the name of newly predicted miRNA. The 'concatenation of the first letter of genus and first two letters of species name of the organism followed by the known homologous miRNA family' is used to assign the nomenclature. Column-3 represents the homologous miRNA of new predicted miRNA. Column-4 to Column-8 comprises the information related to the source organism. Column-9 shows Free energy (ΔG) values for the predicted precursor sequences by RNAfold. (C) Alignment with the global MSA result perspective: In this section, the combined MSA result of 3' UTR belonging to NCBI and GISAID datasets using the respective conserveness (Blue *: NCBI; Green *: GISAID) denotation is shown. The horizontal lines above the SARS-CoV-2 3' UTR bases (29,675–29870) represent its complementary matching region with the respective medicinal plant miRNA along with the site type.

anti-inflammatory and anti-diabetic properties of *P. nigrum* which is commonly used in household as a spice and traditional medicine in many countries other than India. A recent study disclosed the protective role of *P. nigrum* in nasal epithelial barrier dysfunction mostly seen in allergic rhinitis infection [56]. Studies about cross-kingdom approach are quite scarce and to the best of our knowledge, this is the first study to identify miRNA candidates from these three medicinal plants.

The nine conserved nucleotide stretches identified from the MSA results of NCBI and GISAID can act as the potential targets to ensure miRNAs binding. Out of nine, two conserved nucleotide stretches are conserved amongst all 5024 3' UTR of SARS-CoV-2 sequences from 98 region/territories worldwide. The two conserved stretches are (i) TATGGAAGAG and (ii) TAAAATTAAT. Considering that 5–7 bp complementarity between the plant miRNA and its target is sufficient to ensure gene silencing in mammals, we identified a globally conserved target site "GGAAGAG" (NC_045512.2:29,794–29800) in the present study which is a substring of region-i and also present in 5024 3' UTR of SARS-CoV-2 genomes worldwide. This site can effectively function as a common potential target by hsa-miR-1236–3p and predicted *Z. officinale* miRNA zof-miR2673b. These results collectively highlight that this globally conserved target site "GGAAGAG" will enable interaction with both cellular as well as plant miRNA and thereby, targeting this site is crucial to regulate gene expression of the SARS-CoV-2 transcripts. Nucleotide region-ii has not been targeted by any cellular or medicinal plant miRNA. Nonetheless, a perfect complementary artificial miRNA can be synthesized and tested as a candidate. Further, three miRNAs identified from this study belong to the miR477 family suggesting the significant role of these plants against treating SARS-CoV-2 conditions. Hence, the consumption of these medicinal plants either raw or in a decoction on a regular basis might play a substantial role in the prevention or management of the viral disease.

5. Conclusion

Our proposed hypothesis deals with the targeting of the 3' UTR region of SARS-CoV-2 as its miRNA-mediated silencing mechanism could lead to transcriptional repression. Initially, 2656 human mature miRNAs were targeted against the 3' UTR region of the SARS-CoV-2 genome wherein only 19 human miRNAs exhibited the possibility to bind with the viral 3' UTR region. However, such implication of human miRNA does not build up the required anti-viral defense to inhibit viral progression, nevertheless, if this process is aided by exogenous miRNAs, it may build the necessary load of effective miRNAs that could in synergy with existing cellular miRNA bind with 3' UTR and halt viral life cycle. The most widely explored source of exogenous miRNAs is obtained from plant origins. Interaction of such genetic material from different organisms to induce a unique desired effect lays the foundation for cross-kingdom interaction. Our proposed method to search medicinal plant miRNAs concurrently working with human miRNAs to enhance the defense. A total of five candidate miRNAs from three medicinal plants *O. tenuiflorum*, *Z. officinale* and *P. nigrum* were obtained with the potential to target 3' UTR region of SARS-CoV-2. Moreover, the MSA analysis identified one conserved 3' UTR site present in 5024 SARS-CoV-2 genomes targeted by Human miRNA; hsa-miR-1236–3p and predicted *Z. officinale* miRNA; zof-miR2673b. Collectively, this analysis not only

emphasizes the role of these plant miRNAs in improving human defense against viruses but also reveals a conserved region in the SARS-CoV-2 genome that may become a promising target to combat COVID-19.

Funding

The computational analysis in this study was supported by Bioinformatics Node facility provided by Gujarat State Biotechnology Mission (GSBTM), Department of Science & Technology (DST) and Government of Gujarat [grant number GSBTM/MD/JDR/1409/2017–18].

Role of the funding source

The funding sponsors had no role in the study design, in the collection, analysis and interpretation of data; in the writing of the manuscript; and in the decision to submit the manuscript for publication.

Availability of data and material

The additional data is provided in Supplementary material.

Code availability

Not applicable.

CRediT authorship contribution statement

Naman Mangukia: Conceptualization; Methodology; Formal analysis; Data curation; Writing - Original Draft; Writing - review & editing. **Priyashi Rao:** Writing - Original Draft; Writing - review & editing. **Kamlesh Patel:** Supervision. **Himanshu Pandya:** Supervision. **Rakesh M. Rawal:** Conceptualization; Supervision.

Authors approval

All authors have read and approved the final manuscript.

Ethics approval

The manuscript does not contain experiments using animals and does not contain human studies.

Declaration of competing interest

None declared.

Declaration of competing interest

All authors declare no conflict of interest.

Acknowledgement

We dedicate this work to those who are still fighting like a warrior and to those whom we have sadly lost due to this pandemic. Authors thank the invaluable inputs of Mr. Parth Gosai in Graphic designing.

Authors thank Ms. Sukanya Raval and Dr. Prasanth Kumar for proof-reading the manuscript. Author Naman Mangukia acknowledges the Prime Minister's Fellowship (PMF) award from Science and Engineering Research Board (SERB), Department of Science and Technology (DST), Government of India and the Confederation of Indian Industry (CII) and industry support aided by BioInnovations. Authors appreciate the researchers across the globe for sequencing and sharing the complete genome data of SARS-CoV-2 at NCBI and GISAID. The genome sequences used in this study are provided through respective IDs in the supplementary material (NCBI_and_GISAID_Acknowledgement.xls). This entire study is dependent on their precise data.

Appendix A. Supplementary data

Supplementary data to this article can be found online at <https://doi.org/10.1016/j.combiomed.2021.104662>.

References

- N. Zhu, D. Zhang, W. Wang, X. Li, B. Yang, J. Song, J. Zhao, B. Huang, W. Shi, R. Lu, P. Niu, F. Zhan, X. Ma, D. Wang, W. Xu, G. Wu, G.F. Gao, W. Tan, A novel coronavirus from patients with pneumonia in China, 2019, *N. Engl. J. Med.* 382 (2020) 727–733, <https://doi.org/10.1056/nejmoa2001017>.
- P. Rao, A. Shukla, P. Parmar, R.M. Rawal, B.V. Patel, M. Saraf, D. Goswami, Proposing a fungal metabolite-flaviolin as a potential inhibitor of 3CLpro of novel coronavirus SARS-CoV-2 identified using docking and molecular dynamics, *J. Biomol. Struct. Dyn.* (2020) 1–13, <https://doi.org/10.1080/07391102.2020.1813202>, 0.
- C.A. Sariol, L.J. White, Utility, limitations, and future of non-human primates for dengue research and vaccine development, *Front. Immunol.* 5 (2014) 1–15, <https://doi.org/10.3389/fimmu.2014.00452>.
- Y. Zhou, Y. Hou, J. Shen, Y. Huang, W. Martin, F. Cheng, Network-based drug repurposing for novel coronavirus 2019-nCoV/SARS-CoV-2, *Cell Discov* 6 (2020), <https://doi.org/10.1038/s41421-020-0153-3>.
- P. Rao, A. Shukla, P. Parmar, R.M. Rawal, B. Patel, M. Saraf, D. Goswami, Reckoning a fungal metabolite, Pyranonigrin A as a potential Main protease (Mpro) inhibitor of novel SARS-CoV-2 virus identified using docking and molecular dynamics simulation, *Biophys. Chem.* 264 (2020) 106425, <https://doi.org/10.1016/j.bpc.2020.106425>.
- P. Rao, R. Patel, A. Shukla, P. Parmar, R.M. Rawal, M. Saraf, D. Goswami, Identifying structural-functional analogue of GRL0617, the only well-established inhibitor for papain-like protease (PLpro) of SARS-CoV2 from the pool of fungal metabolites using docking and molecular dynamics simulation, *Mol. Divers.* (2021) 1–21, <https://doi.org/10.1007/s11030-021-10220-8>.
- S. Su, G. Wong, W. Shi, J. Liu, A.C.K. Lai, J. Zhou, W. Liu, Y. Bi, G.F. Gao, Epidemiology, genetic recombination, and pathogenesis of coronaviruses, *Trends Microbiol.* 24 (2016) 490–502, <https://doi.org/10.1016/j.tim.2016.03.003>.
- S. Kumar, R. Nyodu, V.K. Maurya, S.K. Saxena, Morphology, genome organization, replication, and pathogenesis of severe acute respiratory syndrome coronavirus 2, (SARS-CoV-2) 2 (2020) 23–31, https://doi.org/10.1007/978-981-15-4814-7_3.
- A. Wu, Y. Peng, B. Huang, X. Ding, X. Wang, P. Niu, J. Meng, Z. Zhu, Z. Zhang, J. Wang, J. Sheng, L. Quan, Z. Xia, W. Tan, G. Cheng, T. Jiang, Genome composition and divergence of the novel coronavirus (2019-nCoV) originating in China, *Cell Host Microbe* 27 (2020) 325–328, <https://doi.org/10.1016/j.chom.2020.02.001>.
- E. Girardi, P. López, S. Pfeffer, On the importance of host MicroRNAs during viral infection, *Front. Genet.* 9 (2018) 1–17, <https://doi.org/10.3389/fgene.2018.00439>.
- D.P. Bartel, MicroRNAs: genomics, biogenesis, mechanism, and function, *Cell* 116 (2004), [https://doi.org/10.1016/S0092-8674\(04\)00045-5](https://doi.org/10.1016/S0092-8674(04)00045-5).
- D.P. Bartel, MicroRNAs: target recognition and regulatory functions, *Cell* 136 (2009) 215–233, <https://doi.org/10.1016/j.cell.2009.01.002>.
- L. Zhang, D. Hou, X. Chen, D. Li, L. Zhu, Y. Zhang, J. Li, Z. Bian, X. Liang, X. Cai, Y. Yin, C. Wang, T. Zhang, D. Zhu, D. Zhang, J. Xu, Q. Chen, Y. Ba, J. Liu, Q. Wang, J. Chen, J. Wang, M. Wang, Q. Zhang, J. Zhang, K. Zen, C.Y. Zhang, Exogenous plant MIR168a specifically targets mammalian LDLRAP1: evidence of cross-kingdom regulation by microRNA, *Cell Res.* 22 (2012) 107–126, <https://doi.org/10.1038/cr.2011.158>.
- V.N. Kim, MicroRNA biogenesis: coordinated cropping and dicing, *Nat. Rev. Mol. Cell Biol.* 6 (2005) 376–385, <https://doi.org/10.1038/nrm1644>.
- B. Wightman, I. Ha, G. Ruvkun, Posttranscriptional regulation of the heterochronic gene *lin-14* by *lin-4* mediates temporal pattern formation in *C. elegans*, *Cell* 75 (1993) 855–862, [https://doi.org/10.1016/0092-8674\(93\)90530-4](https://doi.org/10.1016/0092-8674(93)90530-4).
- S. Griffiths-Jones, H.K. Saini, S. Van Dongen, A.J. Enright, miRBase: tools for microRNA genomics, *Nucleic Acids Res.* 36 (2008) 154–158, <https://doi.org/10.1093/nar/gkm952>.
- A. Kozomara, M. Birgaoanu, S. Griffiths-Jones, MiRBase: from microRNA sequences to function, *Nucleic Acids Res.* 47 (2019) D155–D162, <https://doi.org/10.1093/nar/gky1141>.
- J. Yang, L.M. Farmer, A.A.A. Agyekum, K.D. Hirschi, Detection of dietary plant-based small RNAs in animals, *Cell Res.* 25 (2015) 517–520, <https://doi.org/10.1038/cr.2015.26>.
- Z. Zhou, X. Li, J. Liu, L. Dong, Q. Chen, J. Liu, H. Kong, Q. Zhang, X. Qi, D. Hou, L. Zhang, G. Zhang, Y. Liu, Y. Zhang, J. Li, J. Wang, X. Chen, H. Wang, J. Zhang, H. Chen, K. Zen, C.Y. Zhang, Honeysuckle-encoded atypical microRNA2911 directly targets influenza A viruses, *Cell Res.* 25 (2015) 39–49, <https://doi.org/10.1038/cr.2014.130>.
- S. Zhang, Z. Hong, Mobile RNAs—the magical elf traveling between plant and the associated organisms, *ExRNA* 1 (2019) 4–9, <https://doi.org/10.1186/s41544-019-0007-z>.
- C. Zhao, X. Sun, L. Li, Biogenesis and function of extracellular miRNAs, *ExRNA* 1 (2019) 1–9, <https://doi.org/10.1186/s41544-019-0039-4>.
- L.K. Zhou, Z. Zhou, X.M. Jiang, Y. Zheng, X. Chen, Z. Fu, G. Xiao, C.Y. Zhang, L. K. Zhang, Y. Yi, Absorbed plant MIR2911 in honeysuckle decoction inhibits SARS-CoV-2 replication and accelerates the negative conversion of infected patients, *Cell Discov* 6 (2020) 4–7, <https://doi.org/10.1038/s41421-020-00197-3>.
- O. Safa, M. Hassaniyazad, M. Farashahinejad, P. Davoodian, H. Davdand, S. Hassaniyazad, M. Fathalipour, Effects of Ginger on clinical manifestations and paraclinical features of patients with Severe Acute Respiratory Syndrome due to COVID-19: a structured summary of a study protocol for a randomized controlled trial, *Trials* 21 (2020) 841, <https://doi.org/10.1186/s13063-020-04765-6>.
- J. Alam, T. Hussain, S. Pati, Bio-active compounds (curcumin, allicin and gingerol) of common spices used in Indian and south-east asian countries might protect against COVID-19 infection: a short review, *Eur. J. Med. Plants* (2020) 65–78, <https://doi.org/10.9734/ejmp/2020/v31i2030363>.
- Y. Shu, J. McCauley, GISAID: global initiative on sharing all influenza data – from vision to reality, *Euro Surveill.* 22 (2017) 2–4, <https://doi.org/10.2807/1560-7917.ES.2017.22.13.30494>.
- F. Sievers, A. Wilm, D. Dineen, T.J. Gibson, K. Karplus, W. Li, R. Lopez, H. McWilliam, M. Remmert, J. Söding, J.D. Thompson, D.G. Higgins, Fast, scalable generation of high-quality protein multiple sequence alignments using Clustal Omega, *Mol. Syst. Biol.* 7 (2011), <https://doi.org/10.1038/msb.2011.75>.
- S. Griffiths-Jones, The microRNA registry, *Nucleic Acids Res.* 32 (2004) 109–111, <https://doi.org/10.1093/nar/gkh023>.
- A.J. Enright, B. John, U. Gaul, T. Tuschl, C. Sander, D.S. Marks, MicroRNA targets in *Drosophila*, *Genome Biol.* 5 (2003) R1, <https://doi.org/10.1186/gb-2003-5-1-r1>.
- S.F. Altschul, W. Gish, W. Miller, E.W. Myers, D.J. Lipman, Basic local alignment search tool, *J. Mol. Biol.* 215 (1990) 403–410, [https://doi.org/10.1016/S0022-2836\(05\)80360-2](https://doi.org/10.1016/S0022-2836(05)80360-2).
- C. Camacho, G. Coulouris, V. Avagyan, N. Ma, J. Papadopoulos, K. Bealer, T. Madden, BLAST+: architecture and applications, *BMC Bioinf.* 10 (2009) 421, <https://doi.org/10.1186/1471-2105-10-421>.
- M. Zuker, Mfold web server for nucleic acid folding and hybridization prediction, *Nucleic Acids Res.* 31 (2003) 3406–3415, <https://doi.org/10.1093/nar/gkg595>.
- K. Darty, A. Denise, Y. Ponty, VARNA: interactive drawing and editing of the RNA secondary structure, *Bioinformatics* 25 (2009), <https://doi.org/10.1093/bioinformatics/btp250>, 1974–1975.
- V. Ambros, B. Bartel, D.P. Bartel, C.B. Burge, J.C. Carrington, X. Chen, G. Dreyfuss, S.R. Eddy, S. a M. Griffiths-jones, M. Marshall, M. Matzke, G. Ruvkun, T. Tuschl, T. Le, T.O. Er, THE ED I to R A Uniform System for microRNA Annotation, 2003, pp. 277–279, <https://doi.org/10.1261/rna.2183803.One>.
- R. Sunkar, G. Jagadeeswaran, In silico identification of conserved microRNAs in large number of diverse plant species, *BMC Plant Biol.* 8 (2008) 1–13, <https://doi.org/10.1186/1471-2229-8-37>.
- M. Patel, N. Mangukia, N. Jha, H. Gadhavi, K. Shah, S. Patel, A. Mankad, H. Pandya, R. Rawal, Computational identification of miRNA and their cross kingdom targets from expressed sequence tags of *Ocimum basilicum*, *Mol. Biol. Rep.* 46 (2019) 2979–2995, <https://doi.org/10.1007/s11033-019-04759-x>.
- H. Gadhavi, M. Patel, N. Mangukia, K. Shah, K. Bhadrasha, S.K. Patel, R.M. Rawal, H.A. Pandya, Transcriptome-wide miRNA identification of *Bacopa monnieri*: a cross-kingdom approach, *Plant Signal. Behav.* 15 (2020), <https://doi.org/10.1080/15592324.2019.1699265>.
- N. Jha, N. Mangukia, M.P. Patel, M. Bhavsar, H. Gadhavi, R.M. Rawal, S.K. Patel, Exploring the MiRnome of *Carica papaya*: a cross kingdom approach, *Gene Reports* 23 (2021) 101089, <https://doi.org/10.1016/j.genrep.2021.101089>.
- B.H. Zhang, X.P. Pan, S.B. Cox, G.P. Cobb, T.A. Anderson, Evidence that miRNAs are different from other RNAs, *Cell. Mol. Life Sci.* 63 (2006) 246–254, <https://doi.org/10.1007/s00018-005-5467-7>.
- R. Lorenz, S.H. Bernhart, C. Höner zu Siederdisen, H. Tafer, C. Flamm, P. F. Stadler, I.H. Hofacker, ViennaRNA package 2.0, *Algorithm Mol. Biol.* 6 (2011) 26, <https://doi.org/10.1186/1748-7188-6-26>.
- M. Krzywinski, J. Schein, I. Birol, J. Connors, R. Gascoyne, D. Horsman, S.J. Jones, M.A. Marra, Circos: an information aesthetic for comparative genomics, *Genome Res.* 19 (2009) 1639–1645, <https://doi.org/10.1101/gr.092759.109>.
- R. Lodge, J.A. Ferreira Barbosa, F. Lombard-Vadnais, J.C. Gilmore, A. Deshiere, A. Gosselin, T.R. Wiche Salinas, M.G. Bego, C. Power, J.P. Routy, P. Ancuta, M. J. Tremblay, É.A. Cohen, Host MicroRNAs-221 and -222 inhibit HIV-1 entry in macrophages by targeting the CD4 viral receptor, *Cell Rep.* 21 (2017) 141–153, <https://doi.org/10.1016/j.celrep.2017.09.030>.
- J.L. Smith, S. Jeng, S.K. McWeeney, A.J. Hirsch, A MicroRNA screen identifies the wnt signaling pathway as a regulator of the interferon response during flavivirus infection, *J. Virol.* 91 (2017), <https://doi.org/10.1128/jvi.02388-16>.
- Q. Li, B. Lowey, C. Sodroski, S. Krishnamurthy, H. Alao, H. Cha, S. Chiu, R. El-Diwanly, M.G. Ghany, T.J. Liang, Cellular microRNA networks regulate host

- dependency of hepatitis C virus infection, *Nat. Commun.* 8 (2017), <https://doi.org/10.1038/s41467-017-01954-x>.
- [44] Á.L. Pérez-Quintero, R. Neme, A. Zapata, C. López, Plant microRNAs and their role in defense against viruses: a bioinformatics approach, *BMC Plant Biol.* 10 (2010), <https://doi.org/10.1186/1471-2229-10-138>.
- [45] S.R. Liu, J.J. Zhou, C.G. Hu, C.L. Wei, J.Z. Zhang, MicroRNA-mediated gene silencing in plant defense and viral counter-defense, *Front. Microbiol.* 8 (2017) 1–12, <https://doi.org/10.3389/fmicb.2017.01801>.
- [46] Q.W. Niu, S.S. Lin, J.L. Reyes, K.C. Chen, H.W. Wu, S.D. Yeh, N.H. Chua, Expression of artificial microRNAs in transgenic *Arabidopsis thaliana* confers virus resistance, *Nat. Biotechnol.* 24 (2006) 1420–1428, <https://doi.org/10.1038/nbt1255>.
- [47] S.S. Lin, H.W. Wu, S.F. Elena, K.C. Chen, Q.W. Niu, S.D. Yeh, C.C. Chen, N.H. Chua, Molecular evolution of a viral non-coding sequence under the selective pressure of amiRNA-mediated silencing, *PLoS Pathog.* 5 (2009), <https://doi.org/10.1371/journal.ppat.1000312>.
- [48] C.-G. Duan, C.-H. Wang, R.-X. Fang, H.-S. Guo, Artificial MicroRNAs highly accessible to targets confer efficient virus resistance in plants, *J. Virol.* 82 (2008) 11084–11095, <https://doi.org/10.1128/jvi.01377-08>.
- [49] J. Wu, R. Yang, Z. Yang, S. Yao, S. Zhao, Y. Wang, P. Li, X. Song, L. Jin, T. Zhou, Y. Lan, L. Xie, X. Zhou, C. Chu, Y. Qi, X. Cao, Y. Li, ROS accumulation and antiviral defence control by microRNA528 in rice, *Native Plants* 3 (2017), <https://doi.org/10.1038/nplants.2016.203>.
- [50] A. Gheware, R. Rani, Ad hatoda Vasica : a potential ayurvedic intervention against COVID- 19 associated impaired immune response and hypoxia- in ammatation phenotype, (n.d.) 1–12.
- [51] J. Zheng, Y. Zhou, Y. Li, D.P. Xu, S. Li, H. Bin Li, Spices for prevention and treatment of cancers, *Nutrients* 8 (2016), <https://doi.org/10.3390/nu8080495>.
- [52] R.A. Kulkarni, A.R. Deshpande, Anti-inflammatory and antioxidant effect of ginger in tuberculosis, *J. Compl. Integr. Med.* 13 (2016) 201–206, <https://doi.org/10.1515/jcim-2015-0032>.
- [53] S.S. Ghoke, R. Sood, N. Kumar, A.K. Pateriya, S. Bhatia, A. Mishra, R. Dixit, V. K. Singh, D.N. Desai, D.D. Kulkarni, U. Dimri, V.P. Singh, Evaluation of antiviral activity of *Ocimum sanctum* and *Acacia arabica* leaves extracts against H9N2 virus using embryonated chicken egg model, *BMC Compl. Alternative Med.* 18 (2018) 1–10, <https://doi.org/10.1186/s12906-018-2238-1>.
- [54] S. Kaushik, G. Jangra, V. Kundu, J.P. Yadav, S. Kaushik, Anti-viral activity of *Zingiber officinale* (Ginger) ingredients against the Chikungunya virus, *VirusDisease* 31 (2020) 270–276, <https://doi.org/10.1007/s13337-020-00584-0>.
- [55] J.S. Chang, K.C. Wang, C.F. Yeh, D.E. Shieh, L.C. Chiang, Fresh ginger (*Zingiber officinale*) has anti-viral activity against human respiratory syncytial virus in human respiratory tract cell lines, *J. Ethnopharmacol.* 145 (2013) 146–151, <https://doi.org/10.1016/j.jep.2012.10.043>.
- [56] T.T. Bui, Y. Fan, C.H. Piao, T. Van Nguyen, D. uk Shin, S.Y. Jung, E. Hyeon, C. H. Song, S.Y. Lee, H.S. Shin, O.H. Chai, Piper Nigrum extract improves OVA-induced nasal epithelial barrier dysfunction via activating Nrf 2/HO-1 signaling, *Cell. Immunol.* 351 (2020) 104035, <https://doi.org/10.1016/j.cellimm.2019.104035>.

Naman Mangukia is a Ph.D. student in Gujarat University and a recipient of Prime Minister Research Fellowship award. He has more than 9 years of industrial experience in NGS technology and machine learning. His main research interests are focused on algorithms, small RNA, machine learning and programming.

Priyashi Rao is a Ph.D. student at Gujarat University, Ahmedabad, India. She is having sound grip in molecular biology wet lab techniques. She is having good hand in docking and molecular dynamics simulation studies.

Kamlesh Patel is an enthusiastic entrepreneur and passionate biotechnologist with extensive knowledge in Life Sciences, Clinical and Applied Sciences. He is an innovative founder and team coordinating professional with expertise in operations management, marketing and business development.

Prof. Himanshu Pandya is a Vice Chancellor of Gujarat University, Ahmedabad, Gujarat, India. With more than 20 years teaching experience, he is heading Department of Biochemistry and Forensic Science in Gujarat University, Ahmedabad. Professor is having expertise in the fields of Horticulture, Plant Biotechnology, Plant physiology, Plant Biochemistry, Bioinformatics, Climate Change and Forensic Science.

Prof. Rakesh Rawal is currently working as Professor at Department of Life Sciences, Food Science and Nutrition, School of Sciences, Gujarat University, Ahmedabad, Gujarat, India. The present focus area is in-silico prediction and validation of cancer models with special reference to leukemia along with cross-kingdom miRNA interference. The author is also involved in Biobanking of tumor tissues and genome analysis using next generation sequencing technology and further bioinformatic analysis of the sequencing results. Previous experience involves as Senior Scientific Officer & Head of Division of Medicinal chemistry & Pharmacogenomics with more than 20 years of experience in the field of cancer research.